

# Planning and Control of Autonomous Underwater Vehicle's Trajectory for its Recovery from a Mobile Submarine Platform

Pedro Martínez\*, José L. Aguirre\*, Mariano Saura\*, Pablo Segado\*, Alberto Luaces#

\* Department of Mechanical Engineering  
Universidad Politécnica de Cartagena  
Doctor Fleming, s/n, 30202 Cartagena, Spain  
[joseluis.aguirre,msaura.sanchez]@upct.es  
[pmi,psc1]@alu.upct.es

# Mechanical Engineering Laboratory  
University of La Coruña  
Mendizábal, s/n, 15403 Ferrol, Spain  
aluaces@udc.es

## ABSTRACT

Autonomous underwater vehicles (AUV) have seen a very strong growth over the last decade and, due to the high performance of submarine electronics and navigation systems, AUV applications grow constantly in many different sectors. Nevertheless, risks associated with their recovery exist, and there is a strong interest in the development of effective methods and algorithms to assist in this complex manoeuvre. In this paper, two algorithms that plan and control the trajectory for the underwater recovery of an AUV from a mobile platform have been developed and implemented: the first one plans the AUV trajectory and velocity to reach the mobile target in specific conditions and, the second one, controls the AUV trajectory to follow the path, while checking errors in position, orientation and velocity. The main characteristic of the trajectory is that it has been defined in relative coordinates with respect to the mobile platform; this offers a number of advantages with respect to global trajectories, as obstacle avoidance while the platform moves. The algorithm effectiveness, applicable to any AUV, has been tested by dynamic simulations of the REMUS100 AUV, considering variations in the following variables: initial position and orientation of the AUV, velocity and trajectory of the mobile platform, and refresh rate of navigation system measurements. From the results, it can be inferred that the developed algorithms are able to plan a trajectory in a wide range of initial conditions and to control the vehicle during the whole trajectory with errors under 0.4 meters in position and 10 degrees in orientation.

**Keywords:** Trajectory planning and control, Autonomous underwater vehicle, Recovery submarine platform, Dynamic simulation

## 1 INTRODUCTION

In the Naval industry, there are two fundamental trends that are developing rapidly: to provide a new generation of submarines with an increased payload capacity, and to increase the safety of personnel by using unmanned vehicles. To this end, the US Master Plan [1] has identified up to nine functions in which an autonomous underwater vehicle (AUV) is superior to a conventional submarine. Among these nine functions, the most important are: Intelligence, Surveillance and Reconnaissance (ISR), Mine, Oceanography and Networks Communication / Navigation.

Advances in underwater electronics, onboard energy management, as well as hardware and software for acquisition, processing and storage of large amounts of information, endow these vehicles with such a high performance that they have caught the attention of different kind of organisations: Army, research centers and private companies, to name a few. Part of these achievements are due to the ability of these vehicles to perform long-distance missions autonomously, as they count on the latest developments in sensors: Inertial Measurement Unit (IMU) to estimate spatial position and orientation, Doppler velocity log (DVL) for the measure of depth, temperature sensor, etc; as well as the most advanced navigation systems: Ultra Short Base Line (USBL) to locate a transmitter unit or Obstacle Avoidance Sonar (OAS). In addition, AUVs have control algorithms that allow them to follow a predefined path loaded on their system.

However, the recovery of AUVs from a mobile platform, which is a very interesting problem nowadays, is not solved despite the mentioned technological advances. This is mainly due to the fact that the waypoints that define the trajectory of the AUV are specified with respect to a non-inertial coordinate system (not useful to define the trajectory to reach a mobile platform), to the narrow ranges in the accuracy of the sensors required to avoid obstacles and prohibited navigation zones, and to the limited bandwidth in underwater communications which significantly reduces the possibilities of an accurate guidance and control of the AUV towards a recovery point.

This paper presents a solution to this problem, based on the planning and control of the trajectories defined in terms of relative positioning with respect to the mobile platform. In this sense, the recovery trajectory can be loaded in the AUV system so that, independently from the movement of the platform, the AUV will reach the recovery point while avoiding the predefined obstacles and forbidden navigation areas. The main objective of this work is to define and describe the developed algorithms for trajectory planning and control on an AUV that must be recovered in a moving platform, and to study the stability of the algorithms under variations in the recovery conditions. To do this, in section 2 the dynamic model of the AUV considered in the simulations is presented, and the algorithms for trajectory planning and control are described, as well as the simulations carried out to evaluate the effectiveness of the implemented algorithms. Finally, section 3 shows the simulation results, and the last two sections include the main conclusions of this work and future developments, respectively.

## 2 MATERIAL AND METHODS

This section describes the dynamic model of the AUV used in the study, the algorithms implemented for trajectory planning and control, and the analysis performed to evaluate the effectiveness of the proposed methods.

### 2.1 Dynamic model of the AUV

The effectiveness of the planning and control algorithms proposed in this paper is evaluated by simulating the dynamics of the AUV in an underwater environment. Without loss of generality, the methodology followed in this section (thoroughly described in [2]) considers the AUV REMUS100 whose dynamic equations can be found in [3].

### 2.2 Trajectory planning

The definition of the trajectory that allows the AUV to reach the mobile target is divided into two phases: check the starting position, and plan the trajectory.

**Check the starting position.** The vehicle, after its mission has been finished, navigates towards the starting zone, whose position and size are perfectly defined with respect to the recovery point. In the simulations carried out in this work, a prismatic zone has been defined: at 100 m behind this reference point, it extends up to 300 m (its length is 200 m), it has a width of 240 m ( $\pm 120$  m) and a height of 80 m, ( $\pm 40$  m). The AUV remains in this area, waiting for a ping call from the platform to indicate the start of the recovery manoeuvre. An array of hydrophones (commercial communication technology USBL -UltraShort Base Line-) in the AUV evaluates its position and orientation relative to the target and whether it is within the recovery starting area. If the AUV is not within that zone, it will navigate towards that zone.

**Trajectory planning.** Considering the current position and direction of the AUV with respect to the platform, the speed at which the AUV must navigate among the different sections of the path, and the speed and trajectory of the moving platform, the AUV runs a path planning algorithm that will allow it to reach the destination, while avoiding certain navigation areas defined previously. This path is defined in three steps (Fig.1):

**Stage 1** ( $\overline{P_0P_1}$ ): layout with clothoids and circular curves (based on road layout [4]) allows the

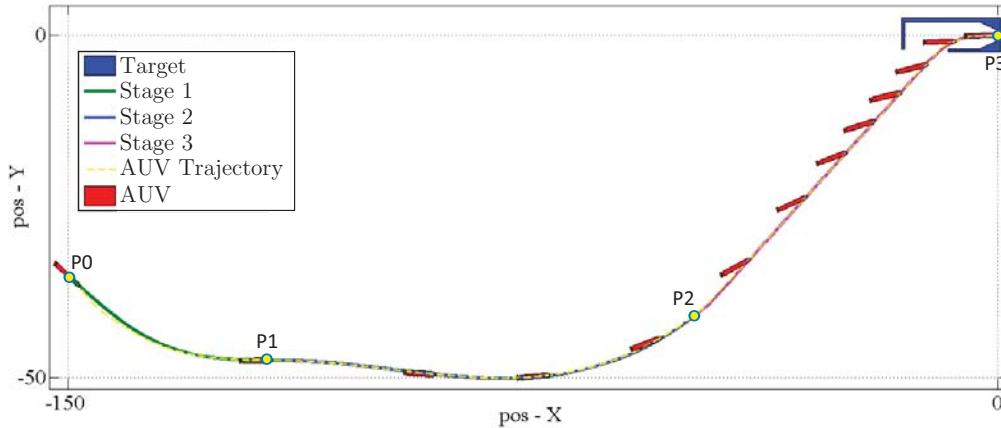


Figure 1: Horizontal view of the three legs of the planned trajectory and the real trajectory followed by the AUV when the target was moving at the speed of 1 knot.

AUV to get oriented in the same direction as the target, keeping its depth during all this part of the trajectory.

**Stage 2 ( $\overline{P_1P_2}$ ):** using cubic spline curves, the AUV is directed to a predefined position next to the target and at its same depth (In Fig. 1 only the horizontal view is shown). In this work, this position has been defined at (-48,-41, 0) m relative to the target.

**Stage 3 ( $\overline{P_2P_3}$ ):** defined, in advance, in the horizontal plane through clothoids and circular arcs and with respect to a coordinate system fixed to the target.

The path planning algorithm takes into consideration that the maximum curvature does not exceed that permitted for the AUV. Through dynamic simulation (turning circle manoeuvre) it has been obtained a radius of curvature of 6 m for the REMUS100. In order the AUV to follow the planned trajectory, a number of interpolated waypoints are defined together with the speed that the AUV must have, at these points, relative to the target.

### 2.3 Trajectory control system

The implemented control system acts on the three governing elements of the AUV: pitch rudder, heading rudder and propulsion system, depending on the errors in position, orientation and velocity calculated by comparing the values obtained by its navigation systems (IMU + USBL) with the planned values on its path (Fig.2). This control system comprises three basic elements: calculation errors, measurement systems (position, orientation and speed, IMU + USBL), and PID controllers.

**I. Navigation systems: IMU + USBL.** At the times indicated by the refresh rate of the USBL, the control algorithm evaluates the position and orientation of the AUV relative to the platform and adds a random error whose order of magnitude coincides to that of commercial devices ( $0.1^\circ$  and  $0.01\text{m}$  [5]). Out of these refresh intervals, the AUV only uses the IMU to estimate its position and orientation.

The IMU operates constantly. The linear acceleration and angular velocities with respect to local axes, affected by a random error, are integrated to obtain continuous estimates of the position and orientation of the AUV. The 1750-IMU from KVH Industries, Inc. (with errors:  $\pm 2\text{mg}$  and  $\pm 2^\circ/\text{hr}$ ) has been considered for the launched simulations.

**II. Error calculation.** This module determines the errors in position, velocity and orientation of the AUV, from the differences between their values during the planned trajectory and the values estimated by the navigation system of the vehicle (IMU and USBL).

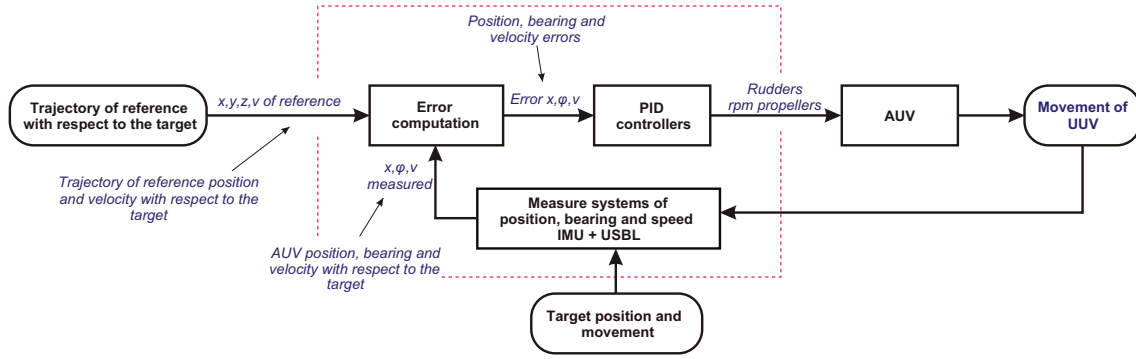


Figure 2: Diagram that shows, together with the AUV dynamic model, the different elements in the control system: calculation errors, measurement systems (IMU + USBL), and PID controllers.

**Position error:** The vertical plane is considered as the one that forms the local vertical axis  $z$  and the line tangent to the trajectory at each point; the horizontal plane is the one that contains this tangent line and is perpendicular to the vertical one. The error in the vertical plane  $|\vec{e}_z(t)|$  is calculated (Eq.2) as the difference in depth between the trajectory point  $(x_i, y_i, z_i)$  and its current estimated position  $(x_{auv}, y_{auv}, z_{auv})$ . In the horizontal plane (Fig.3.a) the position error  $|\vec{e}_h(t)|$  is calculated as the minimum distance between the estimated position of the bow  $(x_{auv}, y_{auv})$ , and the trajectory point  $(x_i, y_i)$ , as shown in Eq. 1.

$$|\vec{e}_h(t)| = [x_{auv} - x_i, y_{auv} - y_i] \quad (1)$$

$$|\vec{e}_z(t)| = [0, z_{auv} - z_i] \quad (2)$$

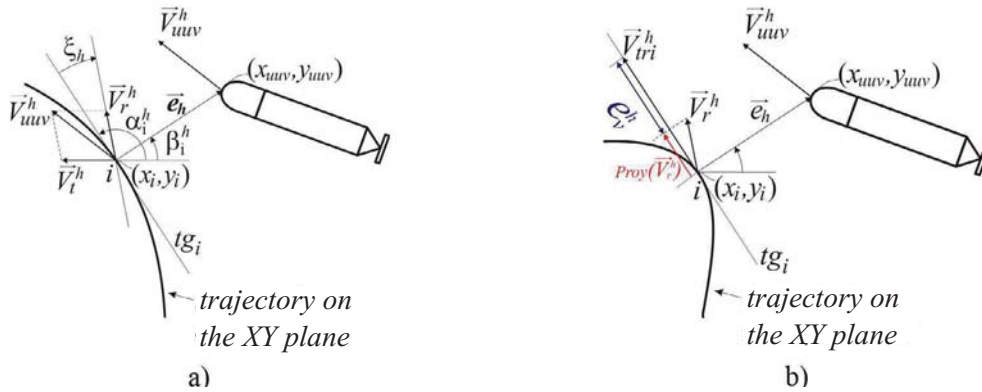


Figure 3: In the horizontal plane it is shown: (a) the variables involved in the position error calculation and, (b) the variables involved in the velocity error calculation.

To strengthen the control system, the trajectory points that the AUV has left behind are no longer considered; that is, if the distance from the bow of the vehicle to the trajectory point  $n$  is larger than the distance to points  $n + 1$  and  $n + 2$ , then point  $n$  is excluded from the trajectory.

**Orientation error:** It is defined as the angular difference between two vectors: the relative velocity of the AUV with respect to the target  $(\vec{V}_r^h)$  and the direction of the vector tangent to the trajectory at the point of minimum distance  $(x_i, y_i)$ , which projected to the horizontal and vertical planes allows us to calculate  $\xi_h(t)$  and  $\xi_z(t)$ , respectively. Figure 3 shows the vectors involved

in the definition of the horizontal orientation error, and Eq.3 shows the analytic expression to calculate it.

$$\xi_h(t) = \arg(\vec{V}_r^h) - \bar{\alpha}_i^h \quad (3)$$

With:

$$\vec{V}_r^h = \vec{V}_{auv}^h - \vec{V}_t^h \quad (4)$$

where:  $\vec{V}_{auv}^h$  is the velocity of the AUV,  $\vec{V}_t^h$  is the velocity of the  $i^{th}$  point of the trajectory and  $\bar{\alpha}_i^h$  is the orientation of vector  $\mathbf{tg}_i$ ; all of them projected to the horizontal plane, which is fixed to the movable target (in all the simulations, this plane coincides with the horizontal plane of the non inertial reference system).

**Velocity error:** Together with the position and orientation errors, it has been defined an error in the velocity of the AUV at which it might reach the target. This error  $e_v$  is calculated (Eq.5) as the difference between the velocity  $\vec{V}_{tri}$  that the AUV might have at each point of the trajectory  $(x_i, y_i)$ , relative to the target, and the projection  $\text{Proy}\vec{V}_r$  of the relative velocity of the vehicle to a vector which is tangent to the trajectory curve at this point. The velocity error is calculated in both the horizontal and the vertical planes of the non inertial coordinate system. The vectors and parameters involved in the horizontal plane are shown in Fig.3.b.

$$\vec{\Delta} = \vec{V}_{tri} - \text{Proy}\vec{V}_r \quad ; \quad e_v = \text{sign}(\vec{\Delta}) * |\vec{\Delta}| \quad (5)$$

#### 2.4 Trajectory control

Three PID controllers (proportional - integral - derivative) act on the orientation of the bearing and pitch rudders, as well as on the rotation speed of the propeller: yaw, pitch and speed of AUV, respectively.

The bearing (yaw) controller evaluates the orientation of the corresponding rudder  $\lambda_{ti}$ , depending on the position  $(|\vec{e}_h|)$  and the orientation  $(\xi_h)$  errors in the horizontal plane, as defined in Eq. 6, where  $K_{pd}$  and  $K_{pa}$  are the proportionality coefficients,  $T_{dd}$  and  $T_{da}$  are derivative time constants, and  $T_{id}$  and  $T_{ia}$  are integral time constants, defined to calculate position errors (subindex **d**) and orientation errors (subindex **a**), respectively. Moreover,  $\alpha$  and  $\beta$  parameters define the distributed weight of both controllers.

$$\begin{aligned} \lambda_{ti} = & \alpha K_{pd} [\text{sign}(\vec{e}_h(t)) |\vec{e}_h(t)| + T_{dd} \text{sign}(\frac{d\vec{e}_h(t)}{dt}) |\frac{d\vec{e}_h(t)}{dt}| + \frac{1}{T_{id}} \int \vec{e}_h(t) dt] + \beta K_{pa} [\xi_h(t) + \\ & + T_{da} \frac{d\xi_h(t)}{dt} + \frac{1}{T_{ia}} \int \xi_h(t) dt] \end{aligned} \quad (6)$$

On the other hand, the pitch controller evaluates the orientation  $\lambda_{ti}^z$  of the corresponding rudder depending on the position  $|\vec{e}_z(t)|$  and orientation  $\xi_z(t)$  errors in the vertical plane, as defined in Eq.7, where:  $K_{pd}^z$  and  $K_{pa}^z$ ;  $T_{dd}^z$  and  $T_{da}^z$ ;  $T_{id}^z$  and  $T_{ia}^z$  and  $\alpha^z$  and  $\beta^z$  have the same meaning than the ones stated for the horizontal plane.

$$\begin{aligned} \lambda_{ti}^z = & \alpha^z K_{pd}^z [\text{sign}(\vec{e}_z(t)) |\vec{e}_z(t)| + T_{dd}^z \text{sign}(\frac{d\vec{e}_z(t)}{dt}) |\frac{d\vec{e}_z(t)}{dt}| + \frac{1}{T_{id}^z} \int \vec{e}_z(t) dt] + \beta^z K_{pa}^z [\xi_z(t) + \\ & + T_{da}^z \frac{d\xi_z(t)}{dt} + \frac{1}{T_{ia}^z} \int \xi_z(t) dt] \end{aligned} \quad (7)$$

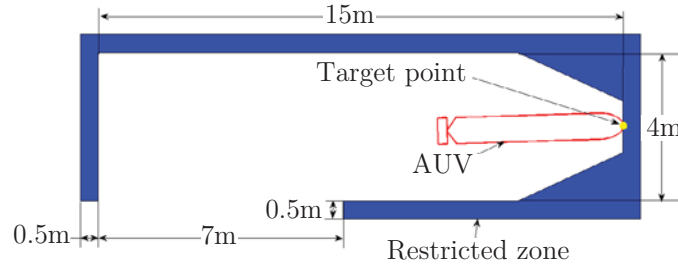


Figure 4: Horizontal view of the cage in which the target point is defined. Shadow zones are forbidden for the navigation of the AUV.

The velocity controller acts over the velocity  $\mathbf{n}_{rpm}$  of the propulsion system (Eq.8), where  $\mathbf{K}_p$ ,  $\mathbf{T}_d$  and  $\mathbf{T}_i$  have the meanings already mentioned.

$$\mathbf{n}_{rpm} = \mathbf{K}_p[\mathbf{e}_v(t) + \mathbf{T}_d \frac{d\mathbf{e}_v(t)}{dt}] + \frac{1}{\mathbf{T}_i} \int \mathbf{e}_v(t) dt \quad (8)$$

All the parameters in Eq.6 - 8 have been tuned by trial and error tests, trying to find a compromise between stability and responsiveness. For the bearing and pitch controllers, the tuning procedure is as follows: in the first place, with the orientation controller deactivated, the position parameters have been tuned by checking that the error along the whole trajectory was minimized. Then we proceeded in reverse order. Finally, the weight distribution of the position and orientation controllers has been determined from the error distribution along the whole trajectory, with special focus on the errors when the target point is reached.

As a final consideration, to achieve a more realistic simulation, kinematic constraints on the rudder movements have been defined: on the one hand, the gyration angle has been limited to  $\pm 20$  degrees, and the angular velocity of the rudders has been limited to rates found in commercial equipment:  $60^\circ$  in 0,2 seconds for the angular velocity of the rudders, and a maximum of 100 rps or 200 rps, at each time step, when increasing or decreasing speed, respectively.

## 2.5 Simulation tests

To evaluate the effectiveness of the algorithms defined in this work, a series of dynamic simulations have been implemented under the Matlab programming environment. The algorithms must be able to plan a trajectory, taking into consideration the limitations of the selected vehicle, so that it can reach a specific target on the mobile platform with the lowest errors in position and orientation, avoiding specific areas in which the navigation of the AUV is forbidden and with the only assistance on its navigation systems: IMU and USBL. To check the effectiveness, different starting positions and orientations, as well as trajectories with different radius of curvature and speeds of the mobile platform, have been considered.

As forbidden navigation areas, the AUV must reach a target point in the interior of a rectangular prism cage with an open lateral access, and whose main dimensions are defined in Fig.4.

Limits for the maximum errors in position ( $\pm 0.4$  m) and orientation ( $\pm 10^\circ$ ) at the target point have been defined. These limits are more restrictive than the values found in the literature for this underwater vehicle [6]. Both the position and orientation errors in the horizontal and the vertical plane will be studied under these conditions: USBL refresh rates (0.1 s and from 0.5 s to 3.0 s with increments of 0.5 s), different velocities (0, 1 and 2 knots) and radius of curvature (100 m, 500 m and  $\infty$ ) of the mobile platform. In all the simulations, commercial errors for the instrumentation USBL and IMU have been already defined:  $\pm 0.1^\circ$ ,  $\pm 0.01$  m and  $\pm 2$  mg,  $\pm 2^\circ/\text{hr}$ , respectively. In order to study the error dispersion, each test has been carried out up to five times.



### 3 SIMULATIONS RESULTS

This section shows and discusses the results obtained from the dynamic simulations that have been carried out.

#### 3.1 Verification of the trajectory planning

Figure 5 shows the capability of the planning algorithm to define the trajectory that the AUV must follow to reach the mobile target. As the position of the AUV within the recovery zone is modified (Fig.5.a), the planning algorithm defines the first and second stages of the trajectory in order to achieve the starting point of the third stage. It can be seen that if this starting point is kept, the third stage remains always the same to ensure that the vehicle does not pass through prohibited navigation areas.

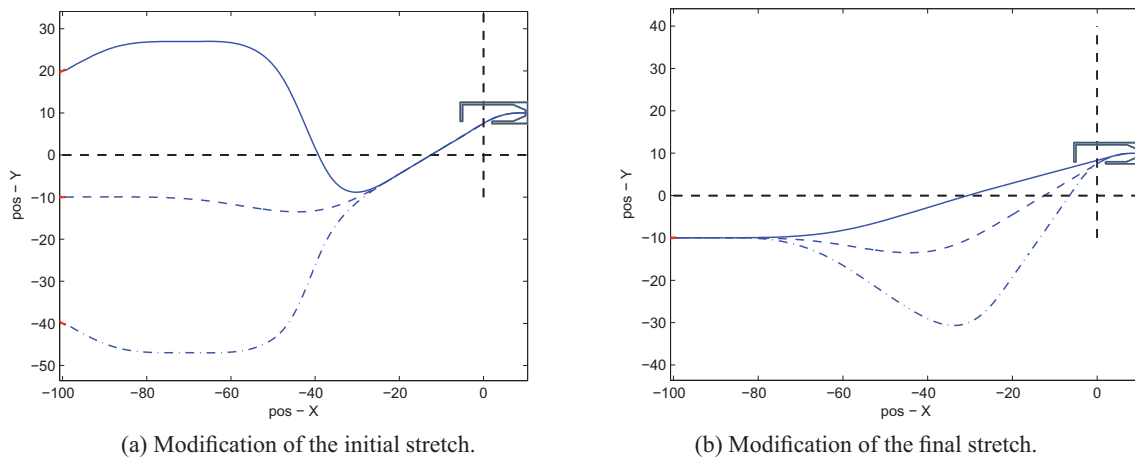


Figure 5: Paths taken by the AUV by modifying different parameters of the trajectory.

On the other hand, Fig. 5.b plots three trajectories planned by the algorithm by keeping fixed the starting position of the recovery manoeuvre, but varying the initial point of the third stage. As shown in the figure, if the point is defined such that the slope of the last stage is very low (solid line), the vehicle might collide with the aft part of the cage. However, even for significantly increased slopes, the AUV will enter in the cage, due to other parameters that define this final step. The entrance curve is determined from the minimum radius of curvature of the vehicle and the maximum centrifugal acceleration experienced by the AUV when it follows the trajectory at a constant speed.

#### 3.2 Path-following errors

Figure 6 shows, as an example, the position and orientation errors of a REMUS100 simulation, both in vertical (pitch) and horizontal (yaw) planes versus the simulation time.

In the position error graph, small oscillations under  $\pm 0.2$  m are shown along the entire path, somewhat higher in yaw at the first stages, because the AUV requires a period of adaptation to meet the target movement conditions.

The bearing error (Figure 6) has a more pronounced oscillation due to the constant adjustment of the aft rudders of the AUV to reduce position and orientation errors. The magnitude of these errors is small ( $\pm 5^\circ$ ), indicating that the controller is fast and robust in sections with different radii of curvature.

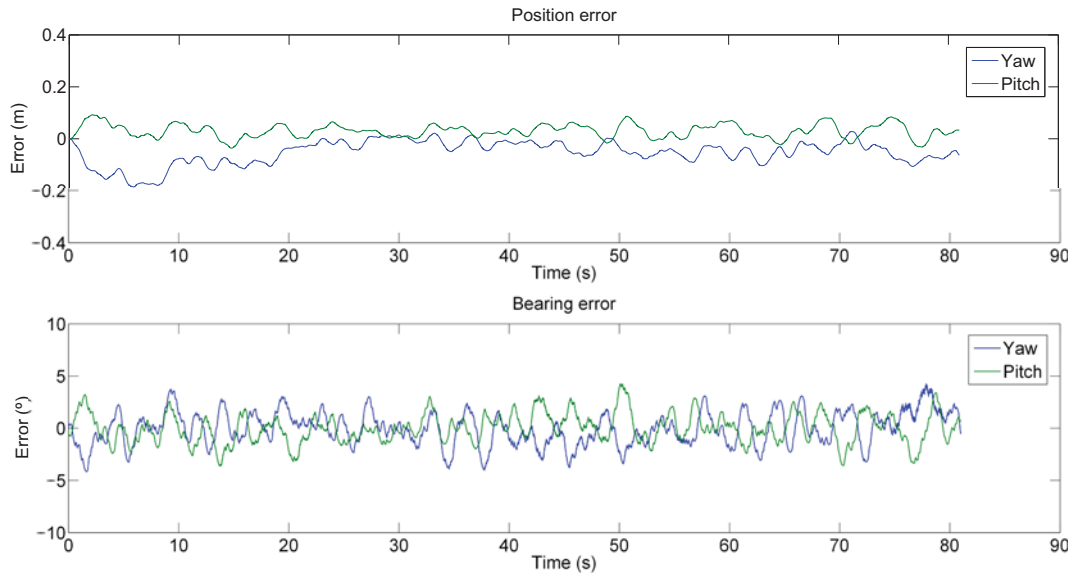


Figure 6: Position and bearing errors, yaw and pitch, of a REMUS100 AUV along the path. Test conditions: USBL refresh time (0.1 s), initial position and orientation of AUV (-110, 20, -20 m) and  $(0^\circ, 0^\circ)$ , target speed (1 knot) and relative arrival speed (0.5 m/s).

### 3.3 Position and bearing errors at the target point

The calculation of the position and bearing errors at the target point allows to evaluate the effectiveness of the developed control algorithms. As indicated in section 2, these errors have been evaluated under different test conditions.

#### Target moving at different velocities

Under the conditions defined in the reference test (section 3.2), in these simulations the target moves in the longitudinal direction at constant speeds: 0, 1 and 2 knots.

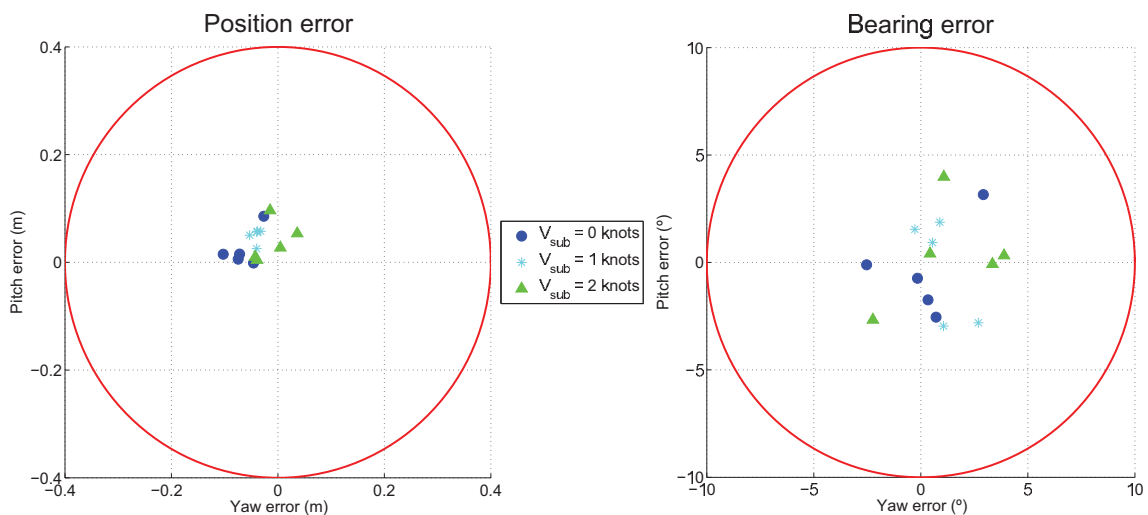


Figure 7: Position and bearing errors of a REMUS100 at the target point under different target velocities.

According to Fig. 7.a, the vehicle is capable of reaching the target area no matter what the platform velocity is, with maximum errors in position around 0.1 m. There is a low dispersion in the results and, the lower the target velocity, the greater the sideways displacement of the error. This is



because, as the relative speed at which the AUV must move is set, the lower is the target velocity, the lower vehicle velocity corresponds and, therefore, the governing capabilities worsen, affecting specially at the stage that drives the AUV into the cage. Furthermore, the definition of a relative path softens the actual path of the AUV as the target velocity increases.

Regarding the bearing error in Fig. 7, the vehicle hits in the target area with a misalignment lower than  $\pm 5^\circ$  for any of the tested velocities. These errors are very small and their dispersion is due to the natural oscillation of the system, as seen in Fig. 6. Nevertheless, it is possible to detect a trend towards a negative yaw misalignment trying to correct the yaw position errors.

### Target moving with different radius of curvature

Maintaining the conditions of the reference test (section 3.2), trajectories of the moving platform are analyzed with the following radius of curvature: 100 m, 500 m and  $\infty$  (straight line). In these tests, the AUV always approaches from the right side of the target which moves at 1 knot and turns to the left side.

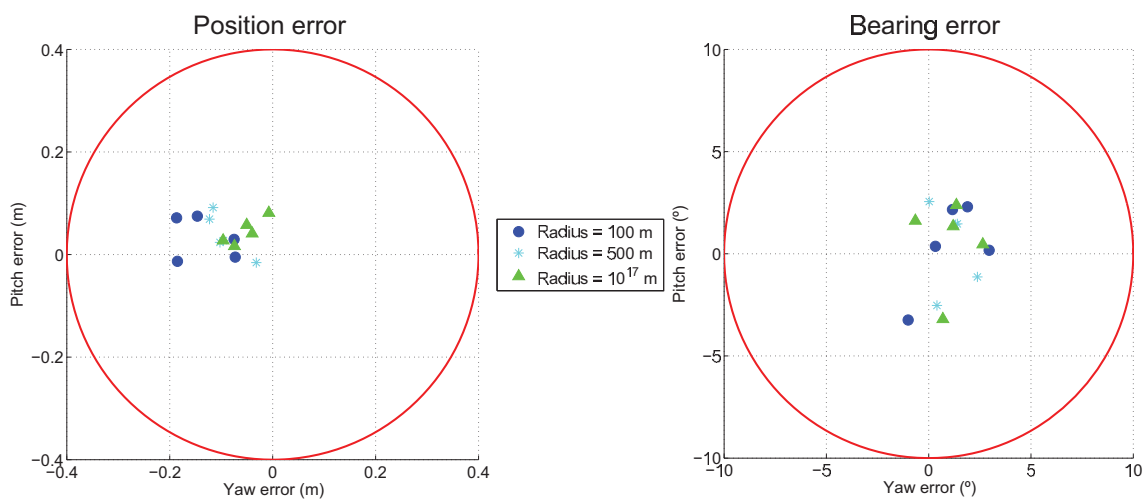


Figure 8: Final position and bearing errors of the REMUS 100 when the target describes three trajectories with different radii of curvature.

Figure 8 shows how the vehicle hits in the target area with less misalignment than  $\pm 5^\circ$  for the radii of curvature considered in the analysis. There is a small dispersion of the errors, which is more pronounced in yaw position and pitch orientation. Although the dispersion in yaw position can be explained because of the major complexity of the approaching manoeuvre as the target trajectory is more closed, the pitch error in orientation varies with independence of the test case. The variations are small, possibly due to instabilities of the AUV equilibrium in the vertical plane.

### 3.4 Different refresh times of the USBL

The AUV uses the IMU to update its position during the navigation, and the error suffers a drift in each iteration step until the USBL refreshes its position and orientation with high accuracy. In this test, maintaining the same reference conditions, the refresh time has been increased until the vehicle fails to hit the target or is unable to follow the path.

In Fig. 9 the vehicle does not hit the target area if the USBL refresh intervals are greater than 3 s. However, no more than  $10^\circ$  misalignment are reached for any test conditions. The dispersion in position error is greater as the refresh rate of USBL signal increases. Additionally, the yaw error is more pronounced when the refresh time is also extended because the trajectory tracking in the last stage worsens, and this affects the AUV arrival.

Regarding the bearing error graph, it should be noted that, although the errors are within the limits

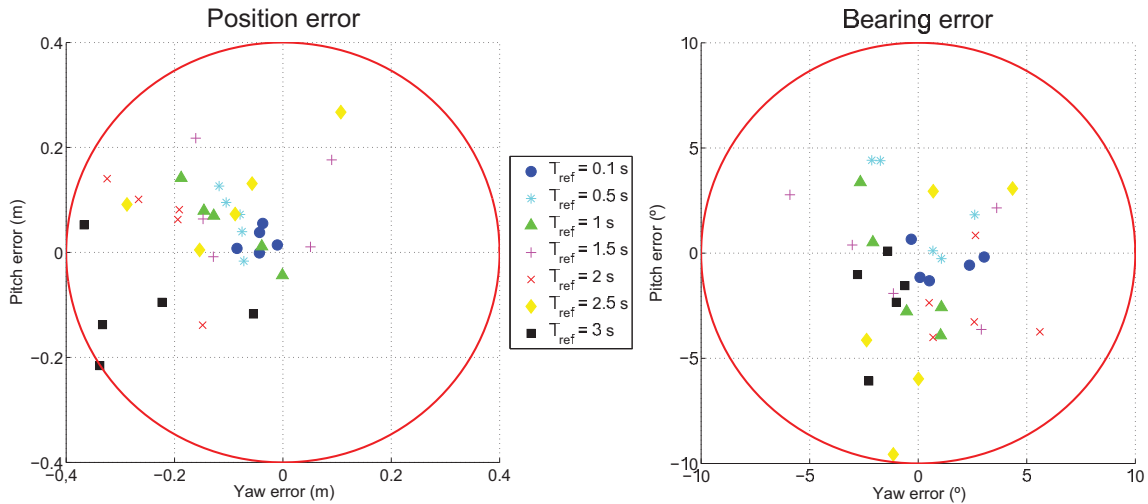


Figure 9: Final position and bearing errors (REMUS100) with different USBL refresh rate.

in all the tests, only 0.1 s and 0.5 s values of refresh rate show a reduced dispersion. Above these values, it is not possible to recognise any variation pattern in the dispersion. A detailed study of the AUV behaviour along the whole trajectory for each refresh rate suggests that this is due to the control characteristics and the update instant of the USBL. When the signal is received on certain sections of the final curve, the system response oscillates slightly, thus producing failures in orientation. However, it has been proved that any attempt to adjust the controller in orientation causes a loss of accuracy in position.

#### 4 CONCLUSIONS

This paper describes the algorithms for trajectory planning and control of an AUV which must pursue a mobile platform and reach a recovery point as accurately as possible in position, orientation and velocity. The trajectory planning algorithm is based on three specific stages which guide the AUV from a remote point, where the recovery manoeuvre starts, to the target point, where it ends; these stages are defined taking into account the vehicle manoeuvrability as well as the velocity and trajectory of the mobile platform. Since the planned trajectory for the AUV is defined relative to the platform, by simply varying the position of the starting point of the third stage, which can be done in advance, the AUV will avoid certain obstacles and prohibited navigation areas whose positions are known with respect to the same reference system.

The control algorithm acts over the depth and the bearing rudders, as well as over the propulsion system to control the pitch, yaw and the speed of the AUV, respectively. These algorithms use a weighted sum of errors, in position and orientation, to determine the angle of the corresponding rudder in the horizontal or the vertical planes. To evaluate these errors, the behaviour of two navigation systems, Inertial Measurement Unit and Ultra Short Base Line, both with commercial accuracies, has been implemented in the control loop.

To evaluate the efficiency of the developed algorithms, a dynamic model of the AUV has been implemented, and several simulations have been run, considering variations in the following parameters: starting point and orientation of the AUV, position and orientation of the AUV at the first point of the third stage, velocity of the AUV relative to the platform, velocity and trajectory of the mobile platform and refresh ratio of the USBL navigation system.

The trajectory planning algorithm defines a trajectory in three sections relative to the mobile platform; this offers the following advantages:

- Independent definition of the last section to ensure that the vehicle reaches the target point

while avoiding obstacles and prohibited navigation areas which are known in advance.

- A more accurate discretization in the last stage than in the other two, as greater AUV navigation restrictions exist, provides a better trajectory tracking and lower position and orientation errors at the target point.
- Precise tracking of the platform regardless of its trajectory and velocity, keeping small deviation in the error values at the recovery point.
- High flexibility in the trajectory definition as a wide range of initial AUV positions and orientations are allowed.

Regarding the adjustment and behavior of the control algorithm, the following conclusions can be drawn:

- Although the horizontal and vertical motion controllers are isolated, no error improvement has been observed when the vehicle moves only on the horizontal plane (first and third stage) with respect to when it moves relative to both of them (second stage).
- The controller parameters have been set by trial and error; although a systematic procedure has been followed, a complex relationship among the three parts (proportional, derivative or integral) makes difficult a perfect tuning of their corresponding parameters.
- It has not been possible to eliminate an oscillation of  $\pm 5^\circ$  in the orientation error along the whole trajectory; however, this error is below the allowable limits defined for a safe recovery.
- Small improvements are obtained in the position accuracy when the linear velocity of the target is increased, and the opposite effect is observed when the turning radius of the target path is reduced. However, despite these variations, in all the simulations the AUV hits the target with high accuracy.
- It has been found that changes in the update time of the USBL signal strongly affects the system accuracy: there is an upper limit of 3 s in the refresh rate. Above this value, the vehicle is unable to reach the target area.

## 5 FUTURE DEVELOPMENTS

During the analysis phase of the simulation results, some ideas have been raised that might improve the system response. With respect to trajectory generation, it has been found that the computational cost can be reduced if, instead of Euler spirals, B-spline curves were used, maintaining a similar behaviour from the point of view of the angular acceleration of the vehicle. In addition, trajectory planning might improve if changes in the velocity of the moving platform were taken into account. Finally, from the point of view of the controller, there are many ways in which it can be improved, as including Kalman filters into the control loop, adaptive control or fuzzy logic strategies, just to mention a few.

## REFERENCES

- [1] “The navy unmanned undersea vehicle (UUV) master plan,” <http://www.navy.mil/navydata/technology/uuvmp.pdf>.
- [2] T. I. Fossen, **Guidance and Control of Ocean Vehicles**. Wiley, 1994.
- [3] T. Presterio, “Verification of a six-degree of freedom simulation model for the REMUS autonomous underwater vehicle,” Master’s thesis, MIT/WHOI, 2001.

- [4] “Instruccion de carreteras,” Norma 3.1-IC. Ministerio de Fomento, Gobierno de España.
- [5] “USBL positioning and communication systems.” EvoLogics. Product information guide 2013.
- [6] T. A. e. a. B. Allen, “Autonomous docking demonstrations with enhanced REMUS technology,” **IEEE Journal of Oceanic Engineering**, 2006.